INTERNATIONAL JOURNAL OF AGRICULTURE & BIOLOGY
ISSN Print: 1560–8530; ISSN Online: 1814–9596
23–0445/2024/31–3–174–182
DOI: 10.17957/IJAB/15.2129
http://www.fspublishers.org

Full Length Article

Analysis of Apoptosis-inducing Effect of Free Fucoxanthin and Fucoxanthin-loaded PLGA Microsphere on Human Lung Cancer H1299 Cell Lines

Dedi Noviendri[1*], Irwandi Jaswir[2], Muhammad Taher[3] and Farahidah Mohammad[3]
[1]*Research Center for Pharmaceutical Ingredients and Traditional Medicine, National Research and Innovation Agency-BRIN. Kawasan Cibinong Science Center, Km 46-Cibinong 16911, Bogor, West Java, Indonesia*
[2]*International Institute for Halal Research and Training (INHART), International Islamic University Malaysia, Jalan Gombak, Kuala Lumpur 53100, Malaysia*
[3]*Department of Pharmaceutical Technology, Faculty of Pharmacy, International Islamic University Malaysia Kuantan, Kuantan 25200, Malaysia*
[*]For Correspondence: dedinov@yahoo.com
Received 25 October 2023; Accepted 21 December 2023; Publishers 14 February 2024

Abstract

Fucoxanthin (FX) has anticancer activity in many different human cell lines. However, this compound was sensitive to light, temperature, poor solubility in water, and low bioavailability. One way to protect FX from rapid degradation was to encapsulate it with PLGA. This study aimed to fabricate FX-loaded microspheres (FX-LMs) using PLGA and to analyze the effects of free FX and FX-LM on the induction of apoptosis in H1299 cells. The results of this study, FX-LM were successfully prepared. The particle size of FX-LM is about 9 µm, and it dissolves completely in water. Free FX showed a high cytotoxic effect on H1299 cells by giving an IC_{50} value of 163.40 μg/mL. However, FX-LM showed a low cytotoxic effect on H1299 cells. The concentration of FX-LM used to test the cytotoxic effect was 1482.50 μg/mL, and the IC_{50} value was not detected. Then, observation of the morphology using a fluorescent microscope showed that H1299 cells treated with free FX and FX-LM appeared irregularly shaped and exhibited several core features of apoptosis. After that, morphological observation by scanning electron microscope showed that H1299 cells treated with free FX and FX-LM showed shrinkage of cells, blebbing of the cell membranes, and formation of apoptosis bodies. Free FX and FX-LM induced caspase-3/7 activation on H1299 cells. Their induced apoptosis was thought to be played by cell mitochondria. In conclusion, free FX was more effective than FX-LM in cytotoxic effects and inducing apoptosis in H1299 cells. These two materials show their potential to prevent lung cancer.

Keywords: Fucoxanthin; PLGA; Apoptosis; Lung cancer; H1299 cells

Introduction

Fucoxanthin (FX) is a xanthophyll specific to brown algae, *Padina australis*, *Turbinaria turbinata*, *Sargassum duplicatum*, and *Sargassum binderi* (Jaswir *et al.* 2011, 2013, 2017; Noviendri *et al.* 2011) that is known to have many biological activities (Chen *et al.* 2022). FX has beneficial medicinal properties for human well-being (Chong *et al.* 2023), including anticancer effects. FX shows good potential for anticancer activity while providing many notable biological activities (Manmuan and Manmuan 2019). This compound had the potential as an agent that prevents cancer in human cell lines such as HL-60 cells (Hosokawa *et al.* 1999), PC-3 cells (Kotake-Nara *et al.* 2005), HepG2 cells (Das *et al.* 2008), MCF-7 cells (Rwigemera *et al.* 2015), SW-620 cells (Manmuan and Manmuan 2019), and A2780 cells (Li *et al.* 2020).

Structurally, FX has a bond of allenic and a 5,6-monoepoxide in its structure (Maeda *et al.* 2018; Cordenonsi *et al.* 2020). This unique structure of FX gives it exceptional biological activity, which is significant for human health enhancement (Zhang *et al.* 2022). The chemical structure of FX is shown in Fig. 1. As described previously, many researchers have studied the activity of FX in cancer treatment, and FX has anticancer activity in many other cell lines of humans. However, this compound has properties that are very sensitive to external environmental influences such as light, temperature, oxygen, acidic pH conditions (Hii *et al.* 2010), poor water solubility, and low bioavailability (Jaiswal *et al.* 2022; Zhang *et al.* 2022). Therefore, we need a treatment that can protect the properties and characteristics of FX compounds so that their ability to bioactivity is not decreased or damaged. One way to protect FX compounds from rapid degradation is to

To cite this paper: Noviendri D, I Jaswir, M Taher, F Mohammad (2024). Analysis of apoptosis-inducing effect of free fucoxanthin and fucoxanthin-loaded PLGA microsphere on human lung cancer H1299 cell lines. *Intl J Agric Biol* 31:174–182

encapsulate them with biodegradable polymers such as PLGA. This polymer has been used to protect bioactive compounds or potential drugs from damage due to external influences. Encapsulation is a promising approach to overcome these challenges by enclosing FX in a protective layer, such as PLGA or microparticles. This way can improve the stability of FX by protecting it from exposure to pH, heat, gastric acids, and enzymes that can accelerate its degradation (Fernandes and Mamatha 2023).

It is worth noting that lung cancer is the second most prevalent type of cancer globally, with breast cancer being the only more common type. This investigation was conducted to explore the impact of FX and its microsphere on lung cancer. The study produced FX-loaded microspheres (FX-LMs) by combining FX with biodegradable PLGA using microencapsulation techniques with a two-step double emulsion extraction/evaporation method (Noviendri *et al*. 2016). The resulting FX-LMs and free FX were then utilized to treat human lung cancer H1299 cell lines.

As far as we know, no prior studies have been performed on the impact of FX entrapped in PLGA on H1299 cells. Then, the mechanisms and effects of free FX (before microencapsulation) and FX-LM (after microencapsulation) inducing apoptosis in H1299 cells remain unclear. Therefore, this study aimed to fabricate an FX-loaded PLGA microsphere (FX-LM) using biodegradable PLGA and polyvinyl alcohol (PVA) and to analyze the effect of free FX (before microencapsulation) and FX-LM (after microencapsulation) in inducing apoptosis in H1299 cells.

Materials and Methods

Materials

The analytical grade of chemicals used in this research, such as phosphate buffer saline/PBS, dichloromethane/DCM (Fisher Scientific, UK), FX 95% purity, and 3-(4,5-dimethyl-2-thiazolyl)-2,5-diphenyl-tetrazolium bromide/ MTT (Sigma-Aldric), medium of Dulbecco's Modified Eagle/DMEM, and fetal bovine serum/FBS (Gibco® Invitrogen), PLGA (PDLG 5004 PURAC, Netherlands), penicillin-streptomycin and trypsin-ethylene diamine tetra acetate (Trypsin-EDTA) (Gibco ® Life Technology), polyvinyl alcohol/PVA with molecular weight 115 kDa (BDH lab. supplies, UK), kit of ApoDIRECT InSitu DNA fragmentation assay (Biovision), and kit of Caspase-3/7 (Promega, Madison WI).

Fabrication of FX-LM

FX-LM was fabricated using a specific method, namely a two-step double emulsion extraction/evaporation method based on Noviendri *et al.* (2016). The summary of this method is shown in Fig. 2.

External morphology observation of samples

An SEM observed free FX, PLGA, and FX-LM based on Ismail *et al.* (2012). The free FX, PLGA, and FX-LM photos were captured with a (JEOL, JSM 6700F Model).

Observation of solubility of FX before and after microencapsulation in water

To observe the solubility of free FX, PLGA and FX-LM. Each sample was 2.5 mg and soaked in 2 mL of distilled water in a glass tube. The sample mixture in a glass tube was shaken vigorously for 1 min and then left for 5 min. After 5 min, the solubility of each mixture was observed in the glass tube.

Culture of H1299 cells

DMEM with 10% FBS inactivation and 1% penicillin-streptomycin (Pen-Strep), temperature of 37°C, and 5% CO_2 atmosphere for H1299 cell culture were used. This cell line was courtesy of Associate Professor Dr. Solachuddin JA Ichwan from the Kuantan Faculty of Dentistry-IIUM, Malaysia.

MTT Assay

The MTT assay is based on Jaswir *et al*. (2011) and was used to determine the cytotoxicity of free FX (before microencapsulation), FX-LM (after microencapsulation), and DOX (as a positive control) against H1299 cells. H1299 cells ($1x10^5$ cells/well) were seeded in a 96-well tissue culture plate and incubated for 24 h. After incubation for 24 h, H1299 cells were treated with free FX, FX-LM, and DOX in the same concentration range (1482.50, 741.25, 370.60, 185.30, 92.60, 46.30, 23.15 and 11.60 μg/mL). The next step followed the method of Mosmann (1983). H1299 cell viability was expressed as a percentage of cell viability compared to the control. The H1299 cell viability percentage was calculated based on Averineni *et al.* (2012). This experiment was repeated three times:

$$\text{Cell viability (\%)} = \left[\frac{\text{OD of treated cells (mean)}}{\text{OD of control cells (mean)}}\right] 100\%$$

Finally, the IC_{50} value is calculated, or the concentration value required to inhibit 50% cell viability by the test samples.

Observation of DNA fragmentation with a fluorescence-inverted microscope

A commercial kit ApoDIRECT InSitu DNA fragmentation assay (BioVision) was used to observe the morphological changes of cellular apoptosis in terms of DNA fragmentation. Briefly, H1299 cells in 12-well plates ($2x10^5$ cells/well) were induced with samples such as

free FX (IC_{50} = 163.40 µg/mL), FX-LM (1482.50 µg/mL, IC_{50} not detected), and DOX (IC_{50} = 38.25 µg/mL) for 48 h. All the steps in this study followed the manufacturer's instructions. Next, cell observations (live and apoptotic) were visualized using a fluorescence microscope with a FITC filter.

Observation of morphology with a SEM

H1299 cells (5x105 cells/well) were seeded onto sterile glass coverslips and placed into 6-well plates overnight until they adhered. The cells were treated with samples such as free FX (IC_{50} = 163.40 μg/mL), FX-LM (1482.50 μg/mL, IC_{50} not detected), and DOX (IC_{50} = 38.25 μg/mL). After treatment, the cells were washed with PBS and fixed with 2.5% glutaraldehyde for 3 h. Then, the cells were washed with PBS and post-fixed with 1% osmium tetroxide in cacodylate buffer for 1 hour. The cells were dehydrated with varying percentages of ethanol for 15 mins each, starting with 35% and ending with 100% hexamethyldisilazane. The cells were stored in a desiccator overnight. The cells were then prepared on coverslips coated with gold in Baltec-CED 030, and the morphology of the cells after being treated with free FX, DOX, and FX-LM were analyzed with an SEM (Carl Zeiss Evo® 50, Germany).

Caspase-3/7 activities

The caspase-Glo® 3/7 kit was used to measure caspase-3 and -7 activity based on the protocol recommended by the manufacturer. H1299 cells ($1x10^5$ cells/well) were seeded in a 96-well flat-bottom plate and incubated for 6 h. After 6 h, H1299 cells were treated with free FX (IC_{50} = 163.40 μg/mL), FX-LM (1482.50 μg/mL, IC_{50} not detected), and DOX (IC_{50} = 38.25 µg/mL) were incubated for 48 h. After 48 h, each well added a 10µl of kit of Caspase-Glo 3/7 and incubated for 1 h. In this study, the H1299 cell was treated with dH_2O as a solvent control for DOX and FX-LM. Then, H1299 was treated with ethanol as a solvent control for FX. Luminescence was measured using a luminometer (Luminoskan, Thermo-Scientific). Measurements of mean Relative Light Units (RLU) according to the following equation (Ang *et al*. 2023):

Relative Light Unit (RLU) = $\text{Luminescence}_{(\text{sample})} - \text{Luminescence}_{(\text{blank})}$

According to the following equation the fold change (FC) against the control of negative was calculated:

FC = [(RLU samples or RLU control of positive)/(RLU control of negative)]

Analysis of Statistic

The data of quantitative are expressed as mean ± deviation of standard. Furthermore, Tukey's post hoc analysis of variance (ANOVA) (SPSS Version-20) was used. The result is considered significant if $p < 0.05$.

Results

Surface morphology of free FX (core), PLGA, (coating), and FX-LM (microsphere)

The FX-loaded PLGA microspheres (FX-LMs) were successfully created using the method described by Noviendri *et al.* (2016). The procedure involved using PVA as a dispersant and was found to be suitable for preparing FX-LM. An SEM was used to observe the external morphology of free FX, PLGA, and FX-LM. The results of the observations with an SEM are shown in Fig. 3, which depicts the external morphology of free FX (Fig. 3a and 3A), PLGA (Fig. 3b and 3B), and FX-LM (Fig. 3c and 3C).

Solubility of FX-LM in the water

During an experimental study, we examined the solubility of three different substances in distilled water. The substances were free FX (A), FX-LM (B), and PLGA (C). Our findings are presented in Fig. 4. We observed that free FX particles (indicated by green arrows) remained suspended in the water (Fig. 4A). FX-LM (Fig. 4B), on the other hand, dissolved completely. However, lumps of PLGA settled at the bottom of the glass tube, as shown by the blue arrow in Fig. 4C.

Cytotoxicity effect of free FX (before microencapsulation) and FX-LM (after microencapsulation)

The cytotoxic effects of FX, FX-LM, and DOX (as positive control) were evaluated by MTT assay. This assay produced a curve of cell viability percentage which is plotted against sample concentrations (Fig. 5). In Fig. 5, it can be seen that FX, FX-LM, and DOX exhibited inhibitory effects on H1299 cell proliferation in a concentration-dependent manner. After that, the IC_{50} values of each sample can be determined, except IC_{50} from FX-LM. Free FX and DOX showed a high cytotoxic effect on H1299 cells by giving IC_{50} values of 163.40 and 38.25 μg/mL, respectively. However, the FX-LM showed a low cytotoxic effect on H1299 cells. In this study, the maximum concentration of FX-LM used to assay the cytotoxic effect was 1482.50 μg/mL, and the IC_{50} value was undetectable. Furthermore, FX-LM had a much lower cytotoxic effect against H1299 cells when compared with free FX at equivalent concentrations. For example, at an equivalent concentration of free FX (200 μg/mL), cell viability was around 40% for H1299 cells, whereas at a concentration of FX-LM (200 μg/mL), cell viability was around 85%.

Nuclei morphological observation of H1299 cells by fluorescent microscope

The *ApoDIRECT InSitu* DNA fragmentation kit was used to observe changes in the nuclear morphology of H1299 cells

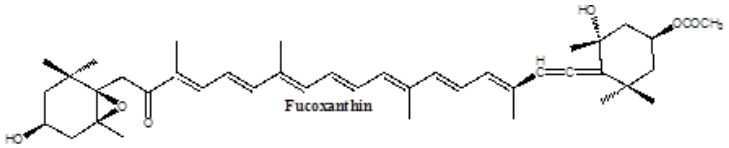

Fig. 1: FX chemical structure

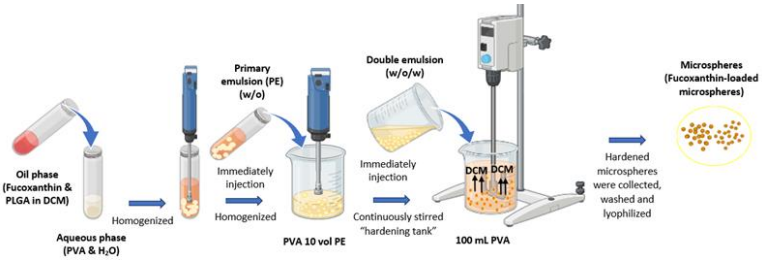

Fig. 2: Technique of microencapsulation with a two-step double emulsion extraction/evaporation method (Noviendri *et al*. 2016)

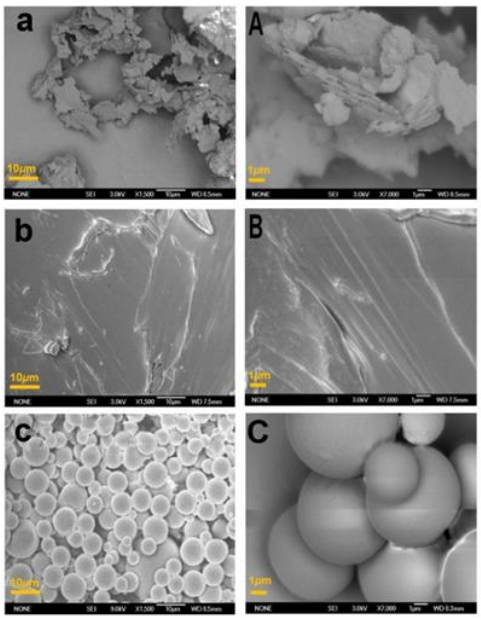

Fig. 3: The image of SEM of FX (a & A), PLGA (b & B), and FX-LM (c & C) with magnification 1500X (small letters: a-c) and 7000X (capital letters: A-C)

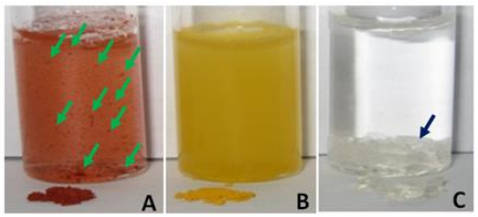

Fig. 4: The solubility of free FX (A), FX-LM (B), and PLGA (C) in the distilled water. Descriptions: the particle of free FX (green arrow) remained suspended in the water, FX-LM dissolved completely in the water, and the lumps of PLGA settled at the bottom of the glass tube (blue arrow)

after being treated with free FX, FX-LM, and DOX. H1299 cells were treated with vehicle (control cells), and the results showed regular cell shape, round cells, and slightly red staining over orange-red propidium iodide (PI) staining indicating healthy nuclear cells (Fig. 6A). However, H1299 cells were treated with free FX (Fig. 6B), DOX (Fig. 6C),

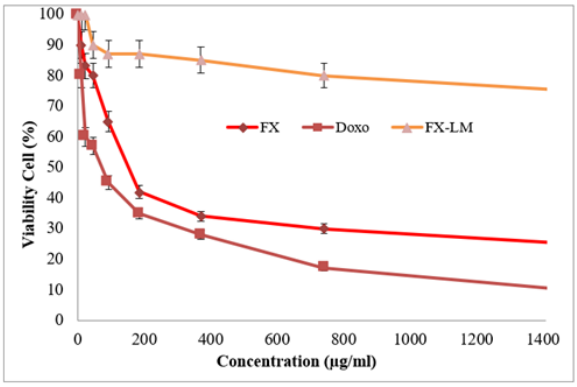

Fig. 5: The concentration-dependent manner of free FX, FX-LM, and DOX on H1299 cells for 48 h

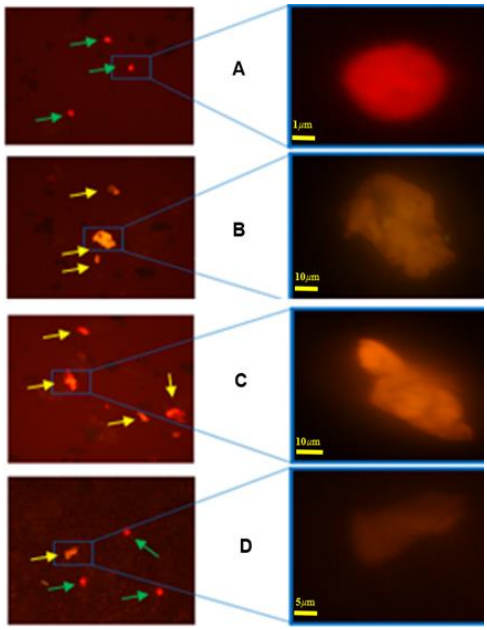

Fig. 6: The images of nuclei morphology by fluorescence microscope of H1299 cells. Untreated cell (control of cell) (A), cell treated with free FX (IC_{50} = 163.40 μg/mL) (B), DOX (IC_{50} = 38.25 μg/mL) (C), and FX-LM (1482.50 μg/mL; IC_{50} not detected) (D). Descriptions: The healthy cells are shown in red (green arrow). The cells of apoptotic are shown in greenish-yellow green (yellow arrow)

and FX-LM (Fig. 6D), and the results showed irregular shapes, non-round cells, and slightly greenish yellow.

Apoptotic features change observation by SEM

Fig. 7A shows the SEM of a vehicle-treated H1299 cell. The result showed a regular shape of the H1299 cell and a normal membranous cell with a smooth cell surface. Then, H1299 cells treated with free FX (IC_{50} = 163.40 µg/mL) (Fig. 7B), DOX (IC_{50} = 38.25 μg/mL) (Fig. 7C), and FX-LM (1482.50 μg/mL; IC_{50} not detected) (Fig. 7D) showed

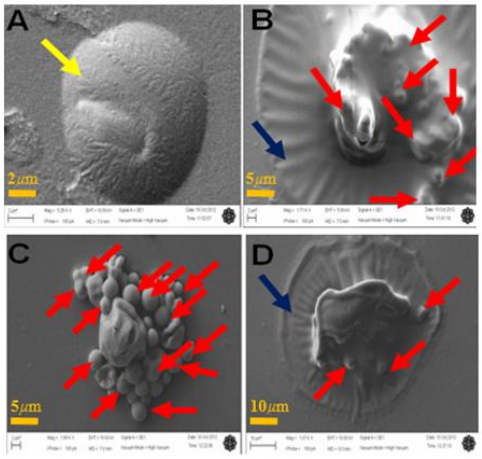

Fig. 7: The image of SEM of H1299 cells. Untreated cell (control of cell) (A), cell treated with free FX (IC_{50} = 163.40 μg/mL) (B), DOX (IC_{50} = 38.25 μg/mL) (C), and FX-LM (1482.50 μg/mL; IC_{50} not detected) (D). Descriptions: The healthy cells are shown a normal membrane of cells with a smooth surface of the cell (yellow arrow). The cells of apoptotic are shown the features of apoptotic cells such as shrinkage of the cell, blebbing of the cell membrane (blue arrow), and apoptotic body formation (red arrows)

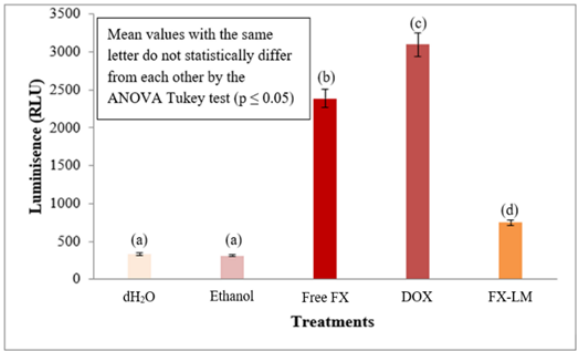

Fig. 8: Caspase-3/7 activities on H1299 cell after treated with free FX (IC_{50} = 163.40 μg/mL), DOX ((IC_{50} = 38.25 μg/mL), and FX-LM (1482.50 μg/mL; IC_{50} not detected)). Description: dH_2O: a control of solvent for DOX and FX-LM; ethanol: a control of solvent for free FX

an irregular shape, cell shrinkage, cell volume decrease, and plasma membrane changes (an abnormal membrane) followed by intense membrane blebbing. The results of this study showed that after 48 h of exposure to free FX, FX-LM, and DOX, H1299 cells exhibited apoptotic morphological features, such as shrinkage of cells, the blebbing of the cell membrane, and the formation of the apoptotic body (Fig. 7B–D).

Furthermore, FX-LM with a concentration of 1482.50 μg/mL, the maximum concentration used in this study, showed a lower apoptosis-inducing effect against the H1299 cell line (Fig. 7D) compared to the effect of free FX (IC_{50} = 163.40 μg/mL) (Fig. 7B). However, H1299 cells treated with DOX (IC_{50} = 38.25 μg/mL) as positive control showed a

higher apoptosis-inducing effect than compared to the effect of free FX and its microsphere on H1299 cells (Fig. 7C).

Caspase-3/7 activities

To investigate the caspase-3/7 activity in the H1299 cell after being treated with free FX, FX-LM, and DOX, the caspase-Glo®3/7 was used. This kit provides the pro-luminescent substrate caspase-3/7 containing the active moiety of the tetrapeptide sequence DEVD for caspase-3 and -7. The H1299 cell treated with FX (IC_{50} = 163.40 µg/mL), FX-LM (1482.50 μg/mL, IC_{50} not detected), and DOX (IC_{50} = 38.25 μg/mL) led to significantly higher ($p < 0.05$) luminescence signal than the vehicle control (dH_2O: a control for DOX and FX-LM; and ethanol: a control for free FX). The values of relative light units (RLU) of free FX, FX-LM, and DOX were 2384.95, 1149.40, and 3095.73 RLU, respectively. Then, the fold change (FC) values of free FX, FX-LM, and DOX were 7.60, 2.20, and 9.30 folds, respectively (Fig. 8).

Discussion

In Fig. 3a and 3A, it can be seen that the external morphology of free FX was in the form of a crystalline solid, while Fig. 3b and 3B show that the external morphology of PLGA was in the form of an amorphous solid. This was following the statement from Yamaguchi *et al.* (2002) reported that in Nature, PLGA was in the form of an amorphous solid. Furthermore, the FX-LMs (Fig. 3c and 3C) with a round, discrete external morphology with a smooth surface, no pores on the surface, no aggregation between microspheres, and a particle size of around 9 μm. This particle size was in line with the results obtained by Jaswir *et al.* (2019), in which the size of the PLGA microsphere containing FX was around 9 μm.

Due to its chemical structure, free FX has limited solubility in water due to its hydroxyl and methyl groups. These features make it less polar and more non-polar, hindering its ability to dissolve in water. According to Chen *et al.* (2022), FX crystals had low water solubility and thus remained insoluble in water. Then, Guler *et al.* (2020) found that free FX did not dissolve in water. However, Shannon and Abu-Ghanna (2018) reported that free FX contains six oxygen atoms in its hydroxyl and epoxy groups. This substance can partially dissolve in polar solvents such as water. Water has unique chemical properties that distinguish it from other substances. The semi-polar characteristic of free FX allows it to dissolve in a mid-polar solvent and easily dissolve in acetone and dimethyl sulfoxide (10 mg/mL). On the other hand, PLGA does not dissolve in water due to its chemical structure, which contains lumps of methyl groups from monomers of lactic acid. These lumps cause the PLGA to settle at the bottom of a glass tube. Wang (2012) also reported that PLGA could be dissolved in solvents such as acetone, tetrahydrofuran, chloroform, ethyl acetate, and dichloromethane. In contrast, FX-LM can be easily dissolved in water due to its chemical composition, which contains hydroxyl groups from polyvinyl alcohol (PVA) (Keegan 2004). PVA acts as a dispersant or emulsifier, which helps to fabricate FX-LM in this study. PVA also acts as a stabilizer to prevent FX-LM from aggregating and settling at the bottom of the solution, preventing the particles from clumping together. These results indicate successful encapsulation of FX, leading to improved solubility and increased bioavailability. Kumagai *et al.* (2018) found that combining FX with gum arabic and γ-cyclodextrin as an emulsifier in water improved the bioavailability of FX. Then, nanoparticles containing FX composed of a combination of chitosan and casein enhanced the effectiveness of FX (Koo *et al*. 2016), and nanoparticles of PLGA-*block*-polyethylene glycol loaded FX (PLGA-PEG-FX) (Yang *et al*. 2021) by making it more bioavailable and water-soluble. Furthermore, Sun *et al.* (2018) reported that FX microcapsules prepared from biopolymers are effective materials. This result is consistent with our results in this study.

In this study, the cytotoxicity effect of free FX, FX-LM, and DOX (as a positive control) against H1299 cells was investigated via MTT assay. This assay was a general method for evaluating the effect of various substances in a cell culture. This assay was used to measure the viability of the cell which is based on the reduction of tetrazolium cleavage into crystals of formazan by an enzyme of mitochondrial dehydrogenase. The MTT assay relies on mitochondrial metabolic activity (Prabst *et al*. 2017). MTT enters the cell into the mitochondria, and then the dehydrogenase enzyme from the mitochondria cleaves the tetrazolium into crystals of formazan. The number of formazan crystals produced was proportional to the living cells number.

Two factors influence the intake of FX-LM on H1299 cells in this study. First is the size of the FX-LM microparticles. Second is the incubation period used to introduce them intact into the cell. The size of the FX-LM was measured to be approximately 9 μm (Fig. 3). This size is considered relatively large enough to infiltrate H1299 cells and make it difficult for them to cross the cell membrane directly. Besides that, 48 h was not enough time for FX release from FX-LM and located intake into the cells. This is due to the continuous release of free FX properties from FX-LM needing much time (more than two days) (data not shown) to be intact in the cells. In other words, it was difficult to penetrate the membrane of H1299 cells directly with FX-LM larger than 1µm. This finding is consistent with the research results of Naha *et al.* (2008, 2012), who stated that particles larger than 1µm may have difficulty passing through cell membranes.

In addition, Mekki *et al.* (2002) have reported that the droplet size of an emulsion significantly influences various factors in cellular lipid uptake. This also applies to the uptake of free FX dependent on lipids (Borel *et al*. 1996). Then, Ravi *et al.* (2018) also reported that combining glycolipids with nanocarriers in chitosan-glycolipid

polymers could increase the cellular uptake and anticancer effect of FX on human colon Caco-2 cells.

To observe the apoptosis induction effect of free FX and DOX in this study, each IC_{50} value was used. The free FX and DOX IC_{50} values were 163.40 and 38.25 µg/mL, respectively. However, the IC_{50} value of FX-LM could not be used in this study because its IC_{50} value was not detected (Fig. 5). Therefore, to observe the apoptosis induction effect of FX-LM, the maximum concentration (1482.50 μg/mL, IC_{50} not detected) used in the MTT assay has been used as a surrogate.

Then, in observations using a fluorescent microscope (Fig. 6) and SEM (Fig. 7), it was seen that free FX and DOX showed a high apoptosis induction effect on H1299 cells (Fig. 6B, 6C; and Fig. 7B, 7C). However, FX-LM showed low apoptosis-induced effects on H1299 cells, and the apoptotic cells number was reduced, as shown in Fig. 6D and Fig. 7D. Later, according to the study conducted by Manmuan and Manmuan (2019), it was found that free FX treatment could cause DNA fragmentation. DNA fragmentation is a hallmark of programmed cell death (Jaleel and Velraj 2022) and a hallmark of apoptosis (Sreejesh and Abraham 2023). This apoptosis process is initially characterized by a series of stereotypic morphological changes (Cohen 1997), such as shrinkage of cells, chromatin fragmentation (Cruchten and Broeck 2002), volume reduction cells (Arends and Wyllie 1991), blebbing of the membrane, and formation of the apoptotic body (Abdelwahab *et al.* 2011). Andraded *et al*. (2010) also reported that the characteristics of apoptosis begin with cell membrane shrinkage and followed by ending with the formation of apoptotic bodies. Furthermore, Takano *et al.* (1991) have also reported that membrane blebbing is a good marker of apoptosis, and membrane blebbing was associated with the formation of the apoptotic ladder.

The changes in apoptotic cell morphology could be observed with microscopes (Barišiĉ *et al*. 2003), such as inverted light microscopes, fluorescent microscopes, and SEM. However, changes in the morphology of apoptotic cells are best seen using SEM (Cruchten and Broeck 2002). In this study, to observe the features of H1299 cell apoptosis induced by free FX, FX-LM, and DOX, a fluorescent microscope (Fig. 6) and an SEM (Carl Zeis Evo® 50, Germany) (Fig. 7) were used.

The caspase-3/7 kit was used to measure the caspase-3/7 activity of free FX (IC_{50} = 163.40 μg/mL), DOX (IC_{50} = 38.25 μg/mL), and FX-LM (1,482.50 μg/mL, IC_{50} not detected) treated on H1299 cells. Fig. 8 showed that the free FX, FX-LM, and DOX induced the caspase-3/7 activation on H1299 cells. Yadav *et al*. (2021) reported that one of the molecular processes demonstrated by apoptotic agents is the activation of caspase-3 or -7.

Then, caspase-3 was the main executioner of apoptosis (Shukla and Nadumane 2021), associated with morphological changes (Hu *et al.* 2021) and associated with apoptosis (Janicke *et al*. 1998). Furthermore, Walsh *et al.* (2008) and Ang *et al*. (2023) reported that caspase-3/7 were downstream effectors of apoptosis that execute cell death. Measurement of caspase-3/7 effector activity is commonly used as a biomarker to assess apoptosis. Kim *et al*. (2010) reported that free FX was crucial in activating the caspase-3 and -7 cleavage process. Finally, from this research, it can be seen from the data of the fluorescent microscope, SEM, and caspase-3/7 activity that free FX, FX-LM, and DOX can induce apoptosis on H1299 cells, which were thought to be played by the cells' mitochondria. This assumption was supported by the data from the MTT assay that has been obtained. This assay is known to be used to measure cell viability, which is based on the reduction of tetrazolium cleavage into formazan crystals by the mitochondrial dehydrogenase enzyme. So, the free FX, DOX, and FX-LM may have induced apoptosis via an intrinsic pathway based on the mitochondria pathway in cells. Gamen *et al*. (2000) reported that the DOX compound was an inducer of apoptosis and was categorized as a mitochondrial pathway in cells.

Conclusion

It can be seen from the fluorescent microscope, SEM, and caspase-3/7 activity data that free FX, FX-LM, and DOX can induce apoptosis in H1299 cells. Their induced apoptosis was thought to be played by cell mitochondria. This assumption is supported by the MTT test data that has been obtained. Furthermore, free FX was more effective than FX-LM in cytotoxic effects and inducing apoptosis in H1299 cells. These two materials show their potential to prevent lung cancer.

Acknowledgments

All authors acknowledge financial support from the Niche Area Fellowship, International Islamic University Malaysia (IIUM), Gombak, Malaysia. No reference: IIUM/503/SA/12/10/4 (2011-2013) and grant RMGS-09-05.

Author Contributions

DN, IJ, and MT planned and designed the experiments; DN, IJ, MT, and FM collected data, statistical analysis of data, and interpreted results; DN and FM made illustrations; DN, IJ, and MT wrote the manuscript.

Conflicts of Interest

All authors declare that there is no conflict of interest in this publication.

Data Availability

The data presented in this publication are available and can be accessed by anyone upon request from the corresponding author.

Ethics Approval

Not applicable to this publication

References

Abdelwahab SI, AB Abdul, S Mohan, MME Taha, S Syam, MY Ibrahim, AA Moriod (2011). Zerumbone induces apoptosis in T-acute lymphoblastic leukemia cells. *Leukem Res* 35:268–271

Andraded R, L Crisol, R Prado, MD Boyano, J Arluzea, J Aréchaga (2010). Plasma membrane and nuclear envelope integrity during the blebbing stage of apoptosis: A time-lapse study. *Biol Cell* 102:25–35

Ang AMG, SRM Tabugo, MM Uy (2023). Antiproliferative, proapoptotic, and antimigration activities of marine sponges against human colon cancer cell line (HCT116). *J Appl Pharm Sci* 13:186–192

Arends MJ, AH Wyllie (1991). Apoptosis: mechanisms and roles in pathology. *Intl Rev Exp Pathol* 32:223–254

Averineni RK, GV Shavi, AK Gurram, PB Deshpande, K Arumugam, N Maliyakkal, SR Meka, U Nayanabhirama (2012). PLGA 50:50 nanoparticles of paclitaxel: Development, in vitro anti-tumor activity in BT-549 cells and in vivo evaluation. *Bull Mater Sci* 35:319–326

Barišiĉ K, J Petrik, L Rumora (2003). Biochemistry of apoptotic cell death. *Acta Pharm* 53:151–164

Borel P, P Grolier, M Armand, A Partier, H Lafont, D Lairon, V Azais-Braesco (1996). Carotenoids in biological emulsions: solubility, surface-to-core distribution, and release from lipid droplets. *J Lipid Res* 37:250–261

Chen Y, N He, T Yang, S Cai, Y Zhang, J Lin, M Huang, W Chen, Y Zhang, Z Hong (2022). Fucoxanthin loaded in palm stearin- and cholesterol-based solid lipid nanoparticle-microcapsules, with improved stability and bioavailability in vivo. *Mar Drug* 20:237

Chong JWR, DYY Tang, HY Leong, KS Khoo, PL Show, KW Chew (2023). Bridging artificial intelligence and fucoxanthin for the recovery and quantification from microalgae. *Bioengineered* 14:1, 2244232, DOI: 10.1080/21655979.2023.2244232

Cohen GM (1997). Caspases: the executioners of the apoptosis. *Biochem J* 326:1–16

Cordenonsi LM, A Santer, RM Sponchiado, NR Wingert, RP Raffin, EES Schapoval (2020). Amazonia products in novel lipid nanoparticles for fucoxanthin encapsulation. *AAPS Pharm Sci Tech* 21:1–10

Cruchten SV, WVD Broeck (2002). Morphological and biochemical aspects of apoptosis, oncosis and necrosis. *Anat Histol Embryol* 31:214–223

Das SK, T Hashimoto, K Kanazawa (2008). Growth inhibition of human hepatic carcinoma HepG2 cells by fucoxanthin is associated with down-regulation of cyclin D. *Biochim Biophys Acta* 1780:743–749

Fernandes V, BS Mamatha (2023). Fucoxanthin, a functional food ingredient: challenges in bioavailability. *Curr Nutr Rep* 12:567–580

Gamen S, A Anel, P Perez-Galan, P Lasierra, D Johnson, A Pineiro, J Naval (2000). Doxorubicin treatment activates a Z-VAD-sensitive caspase, which causes deltapsim loss, caspase-9 activity, and apoptosis in Jurkat cells. *Exp Cell Res* 258:223–235

Guler BA, I Deniz, Z Demirel, O Yesil-Celiktas, E Imamoglu (2020). A novel subcritical fucoxanthin extraction with a biorefinery approach. *Biochem Eng J* 153:107403

Hii S–L, P–Y Choong, K–K Woo, C–L Wong (2010). Stability study of fucoxanthin from *Sargassum binderi*. *Aust J Basic Appl Sci* 4:4580–4584

Hosokawa M, S Wanazaki, K Miyauchi, H Kurihara, H Kohno, J Kawabata, S Odashima, K Takahashi (1999). Apoptosis-inducing effect of fucoxanthin on human leukemia cell line HL-60. *Food Sci Technol Res* 5:243–246

Hu XM, ZX Li, RH Lin, JQ Shan, QW Yu, RX Wang, LS Liao, WT Yan, Z Wang, L Shang, Y Huang, Q Zhang, K Xiong (2021). Guidelines for regulated cell death assays: a systematic summary, a categorical comparison, a prospective. *Front Cell Dev Biol* 9:368

Ismail H, AF Abdalmonemdoolaanea, M Awang, F Mohamed, AFH Ismail (2012). High initial burst release of gentamicin formulated as PLGA microspheres implant for treating orthopaedic infection. *Intl J Pharm Pharm Sci* 4:685–691

Jaiswal J, AK Srivastav, R Patel, U Kumar (2022). Synthesis and physicochemical characterization of rhamnolipid fabricated fucoxanthin loaded bovine serum albumin nanoparticles supported by simulation studies, *J Sci Food Agric* 102:5468–5477

Jaleel A, M Velraj (2022). Petroleum ether extract of *Ophiorrhiza eriantha* Wight induces apoptosis in human breast cancer MCF-7 cell line. *J Appl Pharm Sci* 12:134–142

Janicke RU, MI Sprengart, MR Wati, AG Porter (1998). Caspase-3 is required for DNA fragmentation and morphological changes associated with apoptosis. *J Biol Chem* 273:9357–9360

Jaswir I, D Noviendri, HM Salleh, M Taher, K Miyashita (2011). Isolation of fucoxanthin and fatty acids analysis of *Padina australis* and cytotoxic effect of fucoxanthin on human lung cancer (H1299) cell lines. *Afr J Biotechnol* 10:18855–18862

Jaswir I, D Noviendri, HM Salleh, M Taher, K Miyashita, N RamLi (2013). Analysis of fucoxanthin content and purification of all-trans-fucoxanthin from *Turbinaria turbinata* and *Sargassum plagyophyllum* by SiO_2 open column chromatography and reversed phase-HPLC. *J Liq Chrom Rel Technol* 36:1340–1354

Jaswir I, D Noviendri, M Taher, F Mohamed, HM Salleh, F Octavianti, W Lestari, R Hendri, A Abdullah, K Miyashita, A Hasna (2017). Optimization of essential oil and fucoxanthin extraction from *Sargassum binderi* by supercritical carbon dioxide ($SC\text{-}CO_2$) extraction with ethanol as co-solvent using response surface methodology (RSM). *Intl Food Res J* 24:S514–S521

Jaswir I, D Noviendri, M Taher, F Mohamed, F Octavianti, W Lestari, AG Mukti, S Nirwandar, BBH Almansori (2019). Optimization and formulation of fucoxanthin-loaded microsphere (F-LM) using response surface methodology (rsm) and analysis of its fucoxanthin release profile. *Molecules* 24:947

Keegan ME (2004). *Biodegradable Microspheres with Enhanced Capacity for Surface Ligand Conjugation*. Cornell University, Faculty of the Graduate School, Ithaca, New York. USA

Kim KN, SJ Heo, SM Kang, G Ahn, YJ Jeon (2010). Fucoxanthin induces apoptosis in human leukemia HL-60 cells through a ROS-mediated Bcl-xL pathway. *Toxicol In vitro* 24:1648–1654

Koo SY,I-K Mok, C-H Pan, SM Kim (2016). Preparation of fucoxanthin-loaded nanoparticles composed of casein and chitosan with improved fucoxanthin bioavailability. *J Agric Food Chem* 64:9428–9435

Kotake-Nara E, A Asai, A Nagao (2005). Neoxanthin and fucoxanthin induce apoptosis in PC-3 human prostate cancer cells. *Cancer Lett* 220:75–84

Kumagai K, N Nebashi, A Muromachi, Y Nakano, Y Ito, T Nagasawa (2018). Emulsified fucoxanthin increases stability and absorption in rats. *Nipp Shok Kag Kog Kais* 65:349–356

Li Y, L Tao, L Bao, A Chinnathambi, SA Alharbi, J Cui (2020). Fucoxanthin inhibits cell proliferation and stimulates apoptosis through downregulation of PI3K/AKT/mTOR signaling pathway in human ovarian cancer cells. *Phcog Mag* 16:311–316

Maeda H, S Fukuda, H Izumi, N Saga (2018). Anti-oxidant and fucoxanthin contents of brown alga Ishimozuku (*Sphaerotrichia divaricata*) from the west coast of aomori, Japan. *Mar Drugs* 16:0255

Manmuan S, P Manmuan (2019). Fucoxanthin enhances 5-FU chemotherapeutic efficacy in colorectal cancer cells by affecting MMP-9 invasive proteins, *J Appl Pharm Sci* 9:007–014

Mekki N, M Charbonnier, P Borel, J Leonardi, C Juhel, H Portugal, D Lairon (2002). Butter differs from olive oil and sunflower oil in its effects on postprandial lipemia and triacylglycerol-rich lipoproteins after single mixed meals in healthy young men. *J Nutr* 132:3642–3649

Mosmann T (1983). Rapid colorimetric assay for cellular growth and survival: application to proliferation and cytotoxicity assays. *J Immunol Meth* 63:55–63

Naha PC, V Kanchan, PK Manna, AK Panda (2008). Improved bioavailability of orally delivered insulin using euragit-L30D coated PLGA microparticles. *J Microencapsul* 25:1–9

Naha PC, HJ Byrne, AK Panda (2012). Role of polymeric excipients on controlled release profile of glipizide from PLGA and eudragit RS 100 nanoparticles. *J Nanopharm Drug Del* 1:1–9

Noviendri D, I Jaswir, HM Salleh, M Taher, K Miyashita, N RamLi (2011). Fucoxanthin extraction and fatty acid analysis of *Sargassum binderi* and *S. duplicatum*. *J Med Plants Res* 5:2405–2412

Noviendri D, I Jaswir, M Taher, F Mohamed, HM Salleh, IA Noorbatcha, F Octavianti, W Lestari, R Hendri, H Ahmad, K Miyashita, A Abdullah (2016). Fabrication of fucoxanthin-loaded microsphere (F-LM) by two steps double-emulsion solvent evaporation method and characterization of fucoxanthin before and after microencapsulation. *J Oleo Sci* 65:641–653

Prabst K, H Engelhardt, S Ringgeler, H Hubner (2017). Basic colorimetric proliferation assays: MTT, WST, and Resazurin. *Meth Mol Biol* 1601:1–17

Ravi H, N Kurrey, Y Manabe, T Sugawara, V Baskaran (2018). Polymeric chitosan-glycolipid nanocarriers for an effective delivery of marine carotenoid fucoxanthin for induction of apoptosis in human colon cancer cells (Caco-2 cells). *Mater Sci Eng C Mater Biol Appl* 91:785–795

Rwigemera A, J Mamelona, LJ Martin (2015). Comparative effects between fucoxanthinol and its precursor fucoxanthin on viability and apoptosis of breast cancer cell lines MCF-7 and MDA-MB-231. *Anticancer Res* 35:207–220

Shannon E, N Abu-Ghannam (2018). Enzymatic extraction of fucoxanthin from brown seaweeds. *Intl J Food Sci Technol* 1–10

Shukla M, VK Nadumane (2021). Yellow pigment from a novel bacteria, *Micrococcus terreus*, activates caspases and leads to apoptosis of cervical and liver cancer cell lines. *J Appl Pharm Sci* 11:077–084

Sreejesh PC, A Abraham (2023) Exopolysaccharide from the mice ovarian bacterium *Bacillus velezensis* OM03 triggers caspase- 3-dependent apoptosis in ovarian cancer cells. *J Appl Pharm Sci* 13:154–164

Sun X, Y Xu, L Zhao, H Yan, S Wang, D Wang (2018). The stability and bioaccessibility of fucoxanthin in spray-dried microcapsules based on various biopolymers. *RCS Adv* 8:35138–35149

Takano YS, BV Harmon, JF Kerr (1991). Apoptosis induced by mild hyperthermia in human and murine tumor cell lines: a study using electron microscopy and DNA gel electrophoresis. *J Phatol* 163:329–336

Wang Y (2012). *pH-sensitive and Targeted PLGA-Based Drug Delivery to Colorectal Cancer*. Deakin University, Victoria, Melbourne, Australia

Walsh JG, SP Cullen, C Sheridan, AU Luthi, C Gerner, SJ Martin (2008). Executioner caspase-3 and caspase-7 are functionally distinct proteases. *Proceed Nat Acad Sci USA* 105:12815–12819

Yadav P, R Yadav, S Jain, A Vaidya (2021). Caspase-3: A primary target for natural and synthetic compounds for cancer therapy. *Chem Biol Drug Des* 98:144–65

Yamaguchi Y, M Takenaga, A Kitagawa, Y Ogawa, Y Mizushima, R Igarashi (2002). Insulin-loaded biodegradable PLGA microcapsules: initial burst release controlled by hydrophilic additive. *J Ctrl Rel* 81:235–249

Yang M, L Jin, Z Wu, Y Xie, P Zhang, Q Wang, S Yan, B Chen, H Liang, Naman, J Zhang, S He, X Yan, L Zhao, W Cui (2021). PLGA-PEG nanoparticles facilitate in vivo anti-alzheimer's effects of fucoxanthin, a marine carotenoid derived from edible brown algae. *J Agric Food Chem* 69:9764–9777

Zhang Z, Z Wei, C Xue (2022). Delivery systems for fucoxanthin: research progress, applications and future prospects, *Crit Rev Food Sci Nutr* 15:1–17